Influence of Battery Energy Storage Systems on Transmission Grid Operation With a Significant Share of Variable Renewable Energy Sources

Sérgio F. Santos, Matthew Gough, Desta Z. Fitiwi, André F. P. Silva, Miadreza Shafie-Khah, *Senior Member, IEEE*, and João P. S. Catalão, *Senior Member, IEEE*

***Abstract*—The generation mix of Portugal now contains a significant amount of variable renewable energy sources (RES) and the amount of RES is expected to grow substantially. This has led to concerns being raised regarding the security of the supply of the Portuguese electric system as well as concerns relating to system inertia. Deploying and efficiently using various flexibility options is proposed as a solution to these concerns. Among these flexibility options proposed is the use of battery energy storage systems (BESSs) as well as relaxing system inertia constraints such as the system nonsynchronous penetration (SNSP). This article proposes a stochastic mixed-integer linear programming problem formulation, which examines the effects of deploying BESS in a power system. The model is deployed on a real-world test case and results show that the optimal use of BESS can reduce system costs by as much as 10% relative to a baseline scenario and the costs are reduced further when the SNSP constraint is relaxed. The amount of RES curtailment is also reduced with the increased flexibility of the power system through the use of BESS. Thus, the efficiency of the Portuguese transmission system is greatly increased by the use of flexibility measures, primarily the use of BESS.**

***Index Terms*—Battery energy storage systems (BESSs), renewable energy sources (RES), stochastic mixed-integer linear programming (MILP), system inertia, system nonsynchronous penetration (SNSP), transmission grid operation.**

NOMENCLATURE

A. Sets/Indices

es/Ω^{bess}	Index/set of energy storage.
g/Ω^{g}	Index/set of generators.
h/Ω^{h}	Index/set of hours.
$i,j/\Omega^{i}$	Index/set of buses.
s/Ω^{s}	Index/set of scenarios.
l/Ω^{l}	Index/set of transmission lines.

B. Parameters

$E^{\min}_{es,n,s,h},\ E^{\max}_{es,n,s,h}$	Energy storage limits (MWh).
ER_g	Emission rate (tCO_2e/MWh).
$G_l, B_l,\ S^{\max}_l$	Conductance, susceptance, and flow limit of line l, respectively (Ω^{-1}, Ω^{-1}, MVA).
OC_g	Cost of unit energy production by generator g, (€/MWh).
$p^{\min}_{g,i},\ p^{\max}_{g,i}$	Power generation limits (MW).
$p^{ch,\max}_{es,i},\ p^{dch,\max}_{es,i}$	Charging/discharging limits (MW).
$PD^{i}_{s,h}$	Demand at node (MW).
$R_l,\ X_l$	Resistance and reactance of line l (Ω, Ω).
$\eta^{\text{ch}}_{es},\ \eta^{\text{dch}}_{es}$	Charging/discharging efficiency.
λ^{CO_2}	Cost of emissions (€/tCO_2e).
λ^{es}	Variable price of the storage system (€/MWh).
μ_{es}	Scaling factor (%).
$v^{p}_{s,h}$	Unserved power penalty (€/MWh).
ρ_s	Probability of scenario s.

C. Variables

$E_{es,i,s,h}$	Charge level of BESS (MWh).
$I^{\text{ch}}_{es,i,s,h},\ I^{\text{dch}}_{es,i,s,h}$	Charging/discharging binary variables.
$P_{g,i,s,h}$	Generated power (MW).
$P^{\text{ch}}_{es,i,s,h},\ P^{\text{dch}}_{es,i,s,h}$	Charged/discharged power (MW).
$P^{NS}_{i,s,h}$	Unserved power (MW).
$P_{l,s,h}$	Power flow through a line l (MW).
$PL_{l,s,h}$	Power losses in each line (MW).
$\theta_{l,s,h}$	Voltage angles across the nodes of line l.

D. Functions

TEC	Expected cost of energy (€).
$TENSC$	Expected cost for unserved energy (€).
$TEmiC$	Expected cost of emissions (€).

Manuscript received August 23, 2020; revised December 21, 2020; accepted January 24, 2021. Date of publication February 15, 2021; date of current version March 24, 2022. The work of João P. S. Catalão was supported in part by FEDER funds through COMPETE 2020 and in part by the Portuguese funds through FCT under Grant POCI-010145-FEDER-029803 (02/SAICT/2017). *(Corresponding authors: Miadreza Shafie-khah; João P. S. Catalão.)*

Sérgio F. Santos is with the INESC TEC, Porto 4200-465, Portugal and also with Portucalense University Infante D. Henrique, Porto 4200-072, Portugal (e-mail: sdfsantos@gmail.com).

Matthew Gough is with the Faculty of Engineering, University of Porto and INESC TEC, Porto 4200-465, Portugal (e-mail: mattgough23@gmail.com).

Desta Z. Fitiwi is with the Economic and Social Research Institute, Dublin D02k138, Ireland (e-mail: destinzed@gmail.com).

André F. P. Silva is with the University of Porto, Porto 4200-465, Portugal (e-mail: ec12154@fe.up.pt).

Miadreza Shafie-Khah is with the School of Technology and Innovations, University of Vaasa, 65200 Vaasa, Finland (e-mail: miadreza@gmail.com).

João P. S. Catalão is with the University of Porto and INESC TEC, Porto 4200-465, Portugal (e-mail: catalao@fe.up.pt).

Digital Object Identifier 10.1109/JSYST.2021.3055118

I. INTRODUCTION

A. Motivation, Aims, and Background

OPERATING the electricity transmission network is a complex and crucial task in ensuring that consumers have access to a reliable, efficient, and resilient power supply [1]. This task has become even more complicated with the increasing penetration of renewable energy sources (RESs) [2]. The most

notable sources are solar PV and wind generation [3]. These two generating sources are variable and, thus, introduce additional complexities into transmission grid operations [4]–[6].

Battery energy storage systems (BESSs) can assist in balancing both demand and supply of electricity [7], [8] as well as providing other services to the transmission system operator [9]. Optimally deploying BESS can thus increase the flexibility of power systems [10]. This can lead to higher penetrations of RES in the system [11], [12]. This has led to numerous plans for either 100% RES power systems and, more recently, to an increasing number of plans for full decarbonization of a national economy [13].

This is especially true in the European Union where there is the European Green Deal [14]. This overarching framework requires that the members of the EU transpose this plan to a national level. Portugal has done this through the introduction of a National Climate and Energy Plan, which calls for an economy with net-zero emissions by 2050 [15], [16]. This plan calls for significant increases in RES while reducing the amount of generation derived from combusting fossil fuels [14]. Energy storage systems can play an important enabling role for RES within power systems [17].

The growth of RES envisioned in this plan and the subsequent reduction in traditional thermal generators can create issues related to maintaining adequate rotational inertia in the system [18], [19]. Operating power systems with reduced rotational system inertia are thought to be one of the biggest challenges confronting system operators [18]. Meeting this challenge is a large motivating factor behind this current article.

In addition to being used to decrease the impact of the intermittency associated with RES [20], [21], BESS can also deliver a wide range of services to the network depending on the market structure [22]. The impact of BESS will depend heavily on various characteristics, such as storage capacity, discharge rate, efficiency cycle, lifetime, energy and power density, and cost [8], [23].

The cost of BESS has been falling rapidly and this is allowing wider adoption of these systems [24]. This helps to reduce costs further due to economies of scale and, thus, form a virtuous cycle of increasing deployment and lowering costs [22]. Despite these significant cost reductions, the capital costs of developing BESS projects are significant, and thus, the location and size of BESS should be carefully considered [25].

Within the studies examining the effects of RES on transmission grid operations, stochastic optimization is an efficient and effective tool for problems that involve uncertainty and random variables [26].

Various existing studies have examined the impact of BESS on the stability and flexibility of electric networks.

One of the major concerns of using BESS is the optimal placement and sizing of these systems within the electrical network [22]. Careful site selection of the BESS will increase the reliability and safety of the system as well as minimizing the need for grid investments to maintain and upgrade the network [20], [23], [27].

This optimal site selection will not remove the need for grid enhancements as the BESS may not be able to provide all of the required flexibility and reliability [28]. Thus, a thorough comparison of the use of BESS against the traditional grid investments should be made [29], [30].

In this context, this article presents a new model to investigate the impact of BESS on the operations of transmission systems using a real-world test to provide important results that can be used by system operators, energy regulators, or BESS developers in Portugal. The results of this article can be the basis of policy to increase the penetration of RES within the Portuguese system.

The model incorporates methods to manage uncertainty and operational variability introduced by RES (such as wind and solar) as well as demand. The problem formulated as a mixed-integer linear programming (MILP) model with the specific aims to improve system flexibility, increase RES penetration, reduce losses, and enhance system stability and reliability.

One of the salient features of the new approach presented in our article is the inclusion of the system nonsynchronous penetration (SNSP) restriction so that the system demand is met, which ensures that the system operates within the required frequency and inertia constraints.

B. Literature Review

The impacts of BESS on the operations of transmission grids with high penetrations of RES have been studied by various authors in the past. Several relevant papers have been collected and summarized in Table I.

A paper investigating the effects of BESS in power systems is given in [5], where an MILP model is constructed to examine the effects of widespread integration of RES on the operations of a distribution network. The paper used demand response, energy storage systems, and demand-side resources (including BESS) to increase the flexibility and ability of a distribution network to handle a large amount of RES. The authors focused on the impacts in a distribution network, while this article focuses on the effects on the transmission network.

Yan *et al.* [31] present a comparison between deterministic and robust optimization models to examine the operation of energy storage systems. The objective of the article was to minimize system congestion and the uncertainties associated with the demand, the state of charge (SoC) of the energy storage systems, and renewable energy generation were considered in the robust optimization model. Results from the model show that the energy storage system can increase system flexibility which allows for higher penetrations of renewable energy generation. The users make use of a simplistic representation of an energy storage system and do not consider losses within the power lines.

An MILP-based model to investigate the optimal sizing of BESSs to support renewable energy integration is presented in [22]. The authors show that by combining BESS with a renewable energy plant, the revenues generated from the renewable energy plant are significantly increased. The authors only consider a single plant and do not consider the wider impact of the ESS on the network, including the effects on the losses in the network.

Al Essa [27] develops a framework considering several objectives that aim to assist in power management from renewable energy plants using BESS. The authors consider three objective clusters. The first minimizes the charging cost of the BESS, the

TABLE I
TAXONOMY TABLE OF RELEVANT LITERATURE

Reference	Time frame considered	Type of optimization	Type of energy storage systems	Objective function	Uncertainty considered	Test system	Losses consi-dered	Transmission/Distribution	SNSP
[5]	Operational	MILP	BESS, pumped hydro	Minimize costs	Demand profiles RES generation	IEEE 119 bus	Yes	Distribution	No
[31]	Operational	Robust optimization	BESS	Minimize system congestion	Demand profile, BESS SoC RES generation	Grid supply point UK Distribution system	No	Distribution	No
[22]	Planning	MILP	Li-ion BESS	Maximize NPV	Deterministic	None	No	NA	No
[27]	Operation	MILP	BESS	Minimize: charging cost, charging power, discharging	Deterministic	IEEE 34 bus system	No	Distribution	No
[18]	Operation	MILP	None	Minimize costs	Deterministic	Pan-European	No	Transmission	Yes
[32]	Operation	MILP	None	Minimize costs	Deterministic	Irish single electricity market	No	Transmission	Yes
[33]	Planning	Energy Plan	Pumped hydro	Minimize costs	Demand profiles RES generation	Mainland Portugal	No	Transmission	No
[34]	Planning	MILP	Battery storage	Minimize power loss, costs, emissions	None	Modified 162 distribution system	Yes	Distribution	No
[35]	Planning	Robust optimization	ESS	Minimize cost	RES generation	Garver 6-bus Chinese 196-bus	No	Transmission	No
[36]	Planning	Linear programming	Li-ion BESS	Maximize revenue for the BESS	Locational Marginal Price	IEEE reliability test system	No	Transmission	No
This paper	Operational	MILP	BESS, pumped hydro	Minimize costs	Demand, RE generation	Portuguese network	Yes	Transmission	Yes

Explanation: MILP: Mixed-integer linear programming; BESS: Battery energy storage systems; ESS: Energy storage systems; NPV: Net present value; SoC: State of charge; RES: Renewable energy sources; SNSP: System nonsynchronous penetration.

second minimizes the charging power of the BESS, while the third seeks to minimize the discharging power of the BESS. Results from several scenarios show that the second and third objective clusters can properly manage the BESS to assist in the power management from renewable energy generators. The authors do not consider uncertainty in their model and test on an IEEE 34 test system.

A real-world case study using Portugal was considered by Graça Gomes *et al.* [32] in which the authors present a planning model considering the Portuguese government's National Renewable Energy Action Plan for 2030. The authors present an optimal mix of generators to meet the goals of the Action plan while respecting reliability and security concerns. The authors used existing software to carry out the research and the single objective function aimed to reduce the overall emissions from fossil fuel combustion while respecting various constraints.

Planning energy storage systems located in transmission systems to reduce congestion was carries out in [33].

The authors considered a robust optimization model for the coplanning of ESS and transmission lines and tested the model both on a 6-bus system as well as the 196-bus Chinese system. The authors showed that ESSs become more economical as the distance of the transmission lines increases. The authors did not consider power flow losses within the lines, and this may be important with the long-distance transmission lines that the authors considered.

Bera *et al.* [34] sought to maximize the revenue of a BESS while participating in energy arbitrage and frequency regulation markets. The authors used an improved battery degradation cost but used a simplistic model for the remainder of the BESS constraints. The authors also did not consider losses in the system.

The effects on the operation of power systems as a result of reduced system inertia due to an increase in RES were studied by Mehigan *et al.* [18]. The authors considered a pan-European model with different levels of RES penetration and differing minimum requirements of system inertia through an economic dispatch and unit commitment model. Results showed that increasing the minimum inertia requirements led to increased generation costs, curtailment of RES, and an increase in carbon dioxide emissions. The authors did not consider the impacts of BESS nor did the authors consider system losses, although the authors did use real-world test cases in the modeling and simulation.

Further research into the operational impact of reduced system inertia due to increased RES penetration was carried out by Martin Almenta *et al.* [35]. The authors examine the effects of increased constraints related to the SNSP ratio on the curtailment of wind energy in the Irish single electricity market.

The authors again used a unit commitment and economic dispatch model to show that increasing the limit of SNSP of a power system can reduce the amount of RES curtailment.

The optimal sizing of renewable energy plants and BESS was studied in [36]. The authors propose a novel epsilon multiobjective function to size RES plants as well as BESS according to environmental, technical, and economic aspects. The model is applied to a 162-bus distribution network test case and the results show significant improvements in terms of emissions, project costs, and reduced strain on the grid. The authors considered a metaheuristic algorithm and did not examine the effects of the model on a real-world case study.

Validation of proposed models for BESS integrated generation expansion planning on real-world transmission networks is quite rare.

In a review on generation expansion planning conducted in [29], only six of the 23 models used a test system based on a real-world transmission system and none of the models considered the Portuguese transmission system. The issue of developing models for real-world case studies was also raised by Sinsel *et al.* [4], where the authors state that it is important to examine the relationship between geography and power system characteristics and the types of challenges faced and solutions used in these different power systems. This is done by developing models based on real-world case studies.

Moreover, Table I provides a summary of existing works that are closely related to the present article. This table presents that while numerous studies investigate the impact of BESS on power systems, this article examines important gaps in the literature that have rarely been studied together. This has been done through the use of a stochastic MILP model, which is tested on a real-word transmission system and considers the effect of the BESS on the system operations, and the inclusion of SNSP restriction so that the system demand is met, which ensures that the system operates within the required frequency and maintains adequate rotational inertia in the system. In existing papers, the formulation of the network model is not detailed enough to allow for the calculation of losses during operation. Operating power systems with reduced rotational system inertia is one of the biggest challenges confronting system operators. For the best knowledge of the authors, this analysis of the restriction SNSP in the presence of BESS has not yet been done in any other work in the existing literature. Validation of existing models is rarely done through the use of real-world systems, which is a major contribution of this article. In addition to the influence of the BESS analysis perspective, this article also presents a new optimization model that considers the uncertainty and variability of the renewables and demand.

C. Contributions

This article combines a novel stochastic MILP model to minimize the operational costs of incorporating large-scale storage systems in transmission systems with high levels of renewable energy integration.

This model is tested and validated on a large real-world transmission system, the Portuguese national transmission network.

This article presents the following novel contributions.

1) A stochastic model to assess the long-term benefits of deploying BESSs within the Portuguese Transmission Network.
2) Accurate modeling of the effects of large-scale integration of RES and various flexibility options in real-world power systems through the development of a linear AC-OPF stochastic MILP model. This model provides a good balance between the accuracy of results and computational complexity.
3) Experimental analysis based on numerical results obtained from a real-life system, with the specific aim of improving system flexibility, increasing RES penetration, reduction losses, enhancing system stability, and reliability.
4) The inclusion of the SNSP restrictions helps to increase the accuracy of the scheduling of the required generator dispatch so that the system demand is met, which ensures that the system operates within the required frequency and inertia constraints.

D. Article Layout

The structure of the rest of this article is as follows. Section II contains the mathematical formulation of the problem. Section III presents and discusses the results of the model, while Section IV contains the conclusions.

II. Mathematical Formulation

This section presents the mathematical formulation of the stochastic MILP optimization model that was used in this research. The objective function and the various constraints of the model are described in the following sections.

A. Objective Function

The model sought to minimize the total cost. The total cost was made up of operational costs, costs associated with unserved power, and a cost related to emissions in the system. The total cost is shown as follows:

$$\text{Minimize}\, TC \;=\; \alpha * TEC + \beta * TENSC + \gamma * TEmiC \tag{1}$$

where TC denotes the total operational cost in the system and $\alpha,\ \beta$, and γ are weights that are set at qual initial values. TEC is the expected cost of generating power according to a variety of available technologies (solar PV, wind, large hydro, small hydro, and biomass) as well as expected costs of operating the BESS. The term is given as follows. Degradation costs of the BESS are included.

$$\begin{aligned} TEC = & \sum_{s\in\Omega^s} \rho_s \sum_{h\in\Omega^h} \pi_h \sum_{(g,i)\in\Omega^g} OC_g * P_{g,i,h,s} \\ & + \sum_{s\in\Omega^s} \rho_s \sum_{h\in\Omega^h} \pi_h \sum_{(es,i)\in\Omega^{es}} \lambda_{es} \\ & * \left(P^{\text{dch}}_{es,i,s,h} + P^{\text{ch}}_{es,i,s,h}\right). \end{aligned} \tag{2}$$

The second term *TENSC* in (1) refers to the cost of energy not served due to technical constraints in the system.

This is computed as

$$TENSC \;=\; \sum_{s\in\Omega^s} \rho_s \sum_{h\in\Omega^h} \pi_h \sum_{i\in\Omega^i} \upsilon^P_{s,h} * P^{NS}_{i,s,h}. \tag{3}$$

The term $\upsilon^P_{s,h}$ is defined as a penalty parameter that is correspondent to active power demand shed at a particular time. This parameter must be sufficiently high to avoid an undesirably large amount of unserved power.

Finally, in the last term, $TEmiC$ is responsible for the expected emissions cost in the system. It is a result of power generation and is given as

$$TEmiC \;=\; \sum_{s\in\Omega^s} \rho_s \sum_{h\in\Omega^h} \pi_h \sum_{(g,i)\in\Omega^g} \lambda^{CO_2} * ER_g * P_{g,i,h,s}. \tag{4}$$

B. Constraints

Several constraints are applied to the model, all of which must be satisfied across all operating times to guarantee a safe operation of the transmission network system.

Kirchhoff's current law is the basis for the first constraint and it states that the summation of all injections at a single node should be equal to the summation of all withdrawals at the node. This is applied to the model as follows:

$$\begin{aligned}&\sum_{(g,i)\in\Omega^g} P_{g,i,h,s} + \sum_{(es,i)\in\Omega^{es}} \left(P^{\mathrm{dch}}_{es,i,s,h} - P^{\mathrm{ch}}_{es,i,s,h}\right)\\ &\quad + \sum_{i\in\Omega^{gpt}} \left(P^{\mathrm{HydroPump.}}_{i,s,h} - P^{\mathrm{HydroTurb.}}_{i,s,h}\right)\\ &\quad + P^{NS}_{i,s,h} + \sum_{in,l\in\Omega^l} P_{l,s,h} - \sum_{\mathrm{out},l\in\Omega^l} P_{l,s,h}\\ &= PD^{i}_{s,h} + \sum_{in,l\in\Omega^l} \frac{1}{2} PL_{l,s,h} + \sum_{\mathrm{out},l\in\Omega^l} \frac{1}{2} PL_{l,s,h}\\ &\quad \forall\varsigma\epsilon\Omega^{\varsigma};\ \forall\varsigma\epsilon i; l\epsilon i \end{aligned} \tag{5}$$

The power injected into a node, as described in (5), is composed of the active power delivered by generators, incoming active power along lines connected to the node, discharged power from any BESS, and power generated by using pumped hydro units.

The power being withdrawn at a node is also similarly composed of a number of terms, including, the load demanded at the node, flows of power away along lines, power taken by the BESS to charge, and any power used in the pumped hydro plants for pumping requirements.

Kirchhoff's voltage law provides another constraint. This law governs the power flow associated with any feeder. This law is included in the model by linear approximations of the power flow equations.

The first approximation, which deals with bus voltages being similar to the nominal value (V_{nom}), is valid for transmission systems. The second approximation considers the difference in voltage angles, θ_k. In practice, these values are very small, and thus, the trigonometric expressions are as follows: $\sin\theta_k \approx \theta_k$ and $\cos\theta_k \approx 1$. These two assumptions allow the ac power flow equations to be linearized and the issues related to the nonlinear and nonconvexity of the functions are removed. This then converts the model to a dc power flow model, which is demonstrated as follows:

$$\left|P_{l,s,h} - S_B b_l \theta_{k,s,h}\right| \le MP_l\left(1-u_l\right). \tag{6}$$

The aforementioned equation also includes the state of line u_l, which is represented by a 1 if connected and 0, otherwise. The difference in angles is given by $\theta_{l,s,h} = \theta_{i,s,h} - \theta_{j,s,h}$ with *i* and *j* corresponding to branch *k*. The maximum transfer capacity places *n* upper limit on the power flow in each line. This constraint is shown as follows:

$$P_{l,s,h} \le u_l S^{\max}_l \tag{7}$$

Quadratic functions, as shown in (8), approximate the active power losses. Especially noticeable are the quadratic flow terms that can be easily linearized by performing a piecewise linearization, as shown in [37].

$$PL_{l,s,h} = R_l\, P^2_{l,s,h}\,/S_{B.} \tag{8}$$

Constraints related to BESS are shown in (9)–(14). The limits relating to charging and discharging are shown as follows:

$$0 \le P^{\mathrm{ch}}_{es,i,s,h} \le I^{\mathrm{ch}}_{es,i,s,h} P^{\mathrm{ch,max}}_{es,i,h} \tag{9}$$

$$0 \le P^{\mathrm{dch}}_{es,i,s,h} \le I^{\mathrm{dch}}_{es,i,s,h} P^{\mathrm{ch,max}}_{es,i}. \tag{10}$$

A constraint is added in (11) to ensure that charging and discharging of the BESS cannot take place at the same time. The SoC of the BESS is given by (12).

$$I^{\mathrm{ch}}_{es,i,s,h} + I^{\mathrm{dch}}_{es,i,s,h} \le 1 \tag{11}$$

$$E_{es,i,s,h} = E_{es,i,s,h-1} + \eta^{ch}_{es} P^{\mathrm{ch}}_{es,i,s,h} - P^{\mathrm{dch}}_{es,i,s,h}/\eta^{\mathrm{dch}}_{es}. \tag{12}$$

The SoC of the BESS is limited by lower and upper bounds as follows:

$$E^{\min}_{es,i} \le E_{es,i,s,h} \le E^{\max}_{es,i}. \tag{13}$$

The initial and final SoC need to be determined. In this case, the initial and final SoC are set to be equal to each other. This is shown as follows:

$$E_{es,i,s,h0} = \mu_{es} E^{\max}_{es,i};\ E_{es,i,s,h24} = \mu_{es} E^{\max}_{es,i}. \tag{14}$$

Production of active power by the various generators is limited according to minimum/maximum values as follows:

$$P^{\min}_{g,i,s} \le P_{g,i,h,s} \le P^{\max}_{g,i,s}. \tag{15}$$

The constraints relating to pumped hydro units are presented in (16)–(20). Pumping and energy production are bounded by (16) and (17), respectively

$$0 \le P^{\mathrm{HydroPump.}}_{g,i,s,h} \le I^{\mathrm{HydroPump.}}_{g,i,s,h} P^{\mathrm{HydroPump.,max}}_{g,i,h} \tag{16}$$

$$0 \le P^{\mathrm{HydroTurb}}_{g,i,s,h} \le I^{\mathrm{HydroTurb}}_{g,i,s,h} P^{\mathrm{HydroTurb,max}}_{g,i,h}. \tag{17}$$

Again, a constraint is added to ensure that the pumped hydro unit cannot be pumping and producing power at the same time. This is shown as follows:

$$I^{\mathrm{HydroPump.}}_{g,i,s,h} + I^{\mathrm{HydroTurb}}_{g,i,s,h} \le 1. \tag{18}$$

Bounds are placed on the minimum and maximum levels in the reservoir by the following:

$$Dam2^{\min}_{gt,i} \le E^{\mathrm{HydroPump.}}_{g,i,s,h} \le Dam2^{\max}_{gt,i} \tag{19}$$

$$Dam1^{\min}_{gt,i} \le E^{\mathrm{HydroTurb.}}_{g,i,s,h} \le Dam1^{\max}_{gt,i}. \tag{20}$$

As was the case with the BESS, there are additional constraints relating to the initial and final levels of water in the reservoir are included in the model.

In this article, the frequency and dynamic stability of the system are safeguarded through the SNSP constraint shown in (21). This metric helps to maintain the stability of the power system.

$$\mathrm{SNSP}\ (\%) = \frac{\text{Nonsynchronous generation} + \text{Net interconnetor imports}}{\text{Demand} + \text{Net interconnector exports}} \times 100. \tag{21}$$

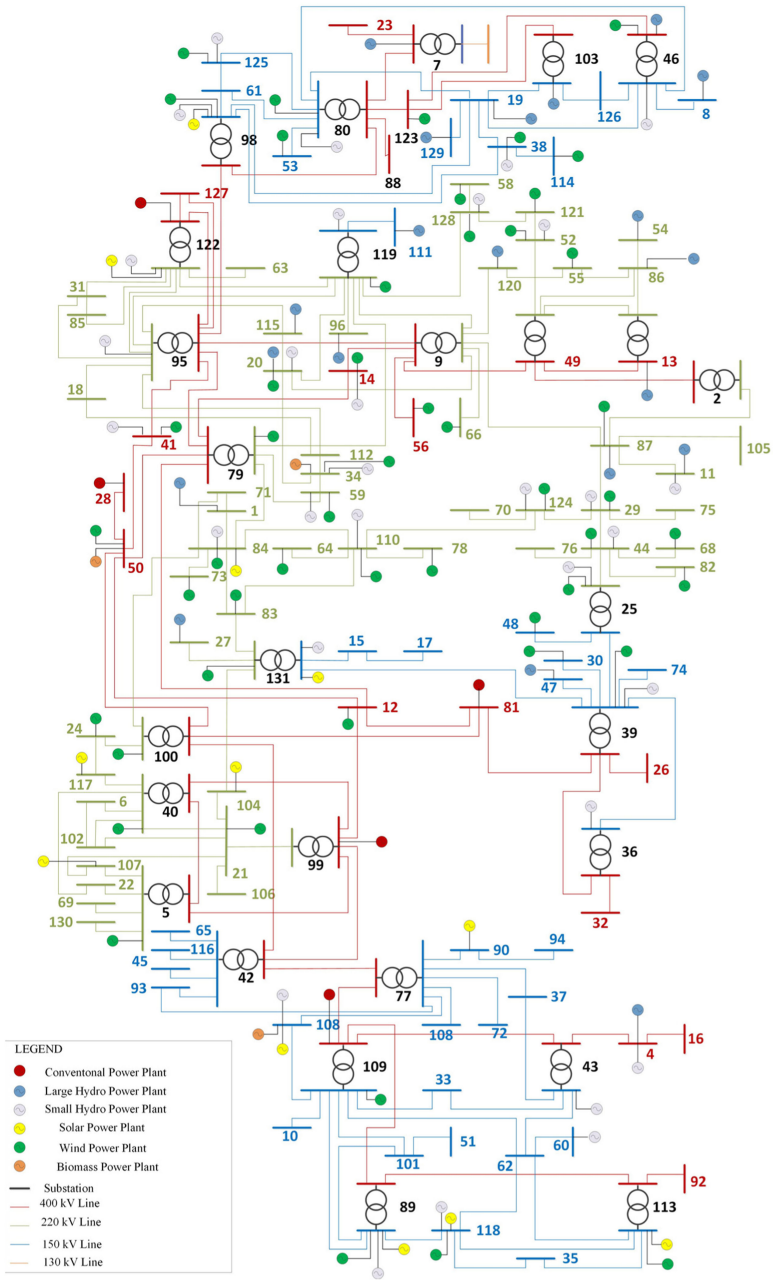

Bus

1 - Aguieira
2 - Aldea da vila (troço português)
3 - Aldea Dávila
4 - Alqueva
5 - Alto de Mira
6 - Alto de São João
7 - Alto Lindoso
8 - Alto Rabagão
9 - Armamar
10 - Artland Sines
11 - Baixo Sabor
12 - Batalha
13 - Bemposta
14 - Bodiosa
15 - Bouçã
16 - Brovales (portuguese section)
17 - Caabril
18 - Canelas
19 - Caniçada
20 - Carrapatelo
21 - Carregado
22 - Carriche
23 - Cartelle (portuguese section)
24 - Carvoira
25 - Castelo Branco
26 - Cedillo (portuguese section)
27 - Castelo de Bode
28 - Lares
29 - Chafariz
30 - Corgas
31 - Custóias
32 - DiVOR2
33 - Ermidas Sado
34 - Estarreja
35 - Estoi
36 - Estremoz
37 - Évora
38 - Fafe
39 - Falagueira
40 - Fanhões
41 - Feira
42 - Fernão Ferro
43 - Ferreira do Alentejo
44 - Ferro
45 - Fogueteiro
46 - Frades
47 - Fratel
48 - Gardunha
49 - Lagoaça
50 - Lavos
51 - Luzianes
52 - Macedo de Cavaleiros
53 - Mendoiro
54 - Miranda
55 - Mogadouro
56 - Moimenta
57 - Monte da Pedra
58 - Montenegrelo
59 - Mourisca
60 - Neves Corvo
61 - Oleiros
62 - Ourique
63 - Ermesinde
64 - Folques
65 - Lusosider
66 - S. Martinho
67 - Conchas
68 - Póvoa
69 - Carnide
70 - Gouveia
71 - Mortágua
72 - Pegões
73 - Pombal
74 - Rodão
75 - Sobral
76 - Fatela
77 - Palmela
78 - Pampilhosa da Serra
79 - Paraimo
80 - Pedralva
81 - Pego
82 - Penamacor
83 - Penela
84 - Pereiros
85 - Perlada
86 - Picote
87 - Pocinho
88 - Ponte de Lima
89 - Portimão
90 - Porto Alto
91 - Zêzere
92 - Puebla de Guzmán (portuguese section)
93 - Quinta do Anjo (AUTO EUROPA)
94 - Quinta Grande
95 - Recarei
96 - Régua
97 - Rerreira do Alentejo
98 - Riba d'Ave
99 - Ribatejo
100 - Rio Maior
101 - Saboia
102 - Sacavém
103 - Salamonde
104 - Santarém
105 - Saucelle
106 - Seixal
107 - Sete Rios
108 - Setúbal
109 - Sines
110 - Tábua
111 - Tabuaço
112 - Tapada do Outeiro
113 - Tavira
114 - Terras Altas de Fafe
115 - Torrão
116 - Trafaria
117 - Trajouce
118 - Tunes
119 - Valdigem
120 - Valeira
121 - Valpaços
122 - Vermoim
123 - Vieira do Minho
124 - Vila Chã
125 - Vila Fria
126 - Vila Nova
127 - Vila Nova de Famalição
128 - Vila Pouca de Aguiar
129 - Vilarinho das Furnas
130 - Zambujal

Fig. 1. Portuguese transmission system.

III. Numerical Results and Discussion

A. Data and Assumptions

A case study that considered the Portuguese Transmission Network was carried out. Data associated with the system were obtained from [38] and [39]. Three voltage levels were modeled 400 kV (red lines), 220 kV (green lines), and 150 kV (blue lines). This system is represented in Fig. 1.

Tables II–VII contain all of the network data as well as the location of generators (both renewable and nonrenewable) [39].

TABLE II
Conventional Generation Data

Node	Node Location	P_max [MW]	Type of Fuel
n28	Lares	826	Gas
n81	Pego	1413	Coal
n99	Ribatejo	1176	Gas
n109	Sines	1180	Coal
n112	Tapada do Outeiro	990	Gas

TABLE III
LARGE HYDRO GENERATION DATA

Node	Node Location	Turbines Mode P_max [MW]	Pumping Mode P_max [MW]
n1	Aguieira	336	273
n4	Alqueva	496	440.4
n7	Alto Lindoso	630	0
n8	Alto Rabagão	68	63.4
n11	Baixo Sabor	189	0
n13	Bemposta	431	0
n19	Caniçada	62	0
n20	Carrapatelo	201	0
n27	Castelo de Bode	159	0
n46	Frades	191	189.4
n47	Fratel	132	0
n54	Miranda	369	0
n86	Picote	440	0
n87	Pocinho	186	0
n96	Régua	180	0
n103	Salamonde	220	0
n111	Tabuaço	58	0
n115	Torrão	140	146.6
n120	Valeira	240	0
n129	Vilarinho das Furnas	62	78.6

TABLE IV
SMALL HYDRO GENERATION DATA

Node	Node Location	P_max [MW]	Node	Node Location	P_max [MW]
n4	Alqueva	13,1	n80	Pedralva	41.5
n14	Bodiosa	40,4	n84	Pereiros	39.1
n20	Carrapate	9,3	n87	Pocinho	9.8
n25	Castelo Branco	2,8	n89	Portimão	2.3
n29	Chafariz	19,8	n95	Recarei	6.2
n34	Estarreja	19,6	n98	Riba d'Ave	45
n36	Estremoz	0,6	n108	Setúbal	30.1
n38	Fafe	27,2	n110	Tábua	3.6
n39	Falagueira	5,2	n118	Tunes	0.6
n41	Feira	4,5	n119	Valdigem	45.5
n43	Ferreira do Alentejo	12,8	n122	Vermoim	1.4
n44	Ferro	58,4	n124	Vila Chã	102.6
n46	Frades	6,7	n125	Vila Fria	16.3
n52	Macedo de Cavaleiros	20,7	n128	Vila Pouca de Aguiar	36.9
n59	Mourisca	17,9	n131	Zêzere	13
n60	Neves Corvo	10,7			

The size of the BESS was set at 100 MW/300 MWh and charging and discharging efficiencies were set at 90%. The peak load in the system is 5384.9 MW.

An operational period of 672 h was used to allow for four representative weeks of the year to be modeled. This is to allow for more accurate simulation of the BESS than the 24-h period, which is usually used.

TABLE V
PV DISTRIBUTED GENERATION DATA

Node	Node Location	P_max [MW]	Node	Node Location	P_max [MW]
n84	Pereiros	4,1	n108	Setúbal	30.1
n89	Portimão	4,4	n113	Tavira	18.4
n90	Porto Alto	16,1	n117	Trajouce	4
n98	Riba d'Ave	2	n118	Tunes	20
n104	Santarém	4,1	n122	Vermoim	2
n107	Sete Rios	1,8	n131	Zêzere	3.7

TABLE VI
WIND DISTRIBUTED GENERATION DATA

Node	Node Location	P_max [MW]	Node	Node Location	P_max [MW]
n5	Alto de Mira	36.4	n66	S. Martinho	275.1
n12	Batalha	122	n68	Póvoa	140
n14	Bodiosa	190.8	n73	Pombal	21.5
n20	Carrapate-lo	216.9	n78	P. Serra+ Toutiço+ V. Grande	258.3
n21	Carregado	17.1	n79	Paraimo	9.7
n24	Carvoira	194.2	n80	Pedralva	14.5
n25	Castelo Branco	38.3	n82	Penamacor	133
n29	Chafariz	258.1	n83	Penela	223.6
n30	Corgas	180.6	n84	Pereiros	125.2
n34	Estarreja	43.9	n87	Pocinho	8.3
n38	Fafe	112.1	n89	Portimão	167.6
n39	Falagueira	57.3	n98	Riba d'Ave	2.2
n40	Fanhões	98.1	n100	Rio Maior	214.4
n41	Feira	43.2	n109	Sines	20.3
n44	Ferro	96.2	n110	Tábua	93.2
n46	Frades	215.8	n113	Tavira	152.6
n48	Gardunha	114	n114	Terras Altas de Fafe	114
n50	Lavos	8.3	n118	Tunes	6.5
n52	Macedo de Cavaleiros	74.6	n119	Valdigem	303.4
n53	Mendoiro	258	n121	Valpaços	53.6
n55	Moga-douro	4.3	n123	Vieira do Minho	240
n56	Moimenta	156.4	n124	Vila Chã	1.3
n58	Monte-negrelo	180	n125	Vila Fria	100.7
n59	Mourisca	34.4	n128	Vila Pouca de Aguiar	116.4
n64	Folques	109.4	n131	Zêzere	41

Large pumped hydro plants are located in Aguieira, Alqueva, Alto Rabagão, Frades, Torrão, and Vilarinho das Furnas. BESS is placed optimally at 13 nodes, which are Castelo Branco, DiVOR, Falagueira, Gardunha, Estoi, Estremoz, Tunes, Carregado, Sacavém, and Ferro.

The chosen nodes are close to areas of large renewable energy generators or dense load centers. The installed capacity of wind power was set to increase by 10% per year for the next 15 years.

Additionally, three scenarios of demand growth were considered; these were constant growth rates of 5%, 10%, and 15% over the next 15 years. Each scenario was given an equal probability of occurrence.

TABLE VII
BIOMASS DISTRIBUTED GENERATION DATA

Node	Node Location	P_max [MW]
n34	Biomassa de Cacia (Estarreja)	47.6
n50	Figueira da Foz (Lavos)	95
n108	Biomassa de Setúbal	66.4

The various demand scenarios were used as a way to model uncertainty. In addition, uncertainty around solar and wind energy production was considered. Each of the three types of uncertainty is accounted for through the use of three scenarios, each with a different hourly profile.

The uncertainty inherent in the wind speed and solar radiation is assumed to cause a $\pm 15\%$ deviation from the average power output profiles of the RES plants. This uncertainty can be caused by a $\pm 5\%$ forecasting error in wind speed or solar radiation.

From these assumptions, two hourly profiles of wind power output are derived. One profile is 15% below the average profile, while in the other, the output is 15% above the average hourly value. These two profiles combined with the average profile led to three wind energy scenarios. A similar procedure is carried out for the solar power output so that there are also three scenarios for this technology (15% below average, average, and 15% above average).

These three sets of hourly profiles are combined to form a set of 27 scenarios that are used in the analysis. Each of the 27 scenarios is assumed to be equally probable.

To ensure the tractability of the problem, the multidimensional input data of size $27*8760$ (27 scenarios for each of the 8760 h in the year) are clustered into groups of size $27*200$ through the use of a k-means clustering algorithm [40]. This means that each cluster is a group of similar operational situations. From these situations, a representative situation is obtained corresponding to the average operational profile in each of the clusters. A weighting is applied to each representative profile following the number of profiles in that group in proportion to the total number of operational cases. While this method ensures the tractability of the problem, it, unfortunately, means that the chronological order of the time series data is not maintained. This means that the level of the autocorrelation of the data cannot be measured. In the context of medium- to long-term planning problems, the loss of this information may not be significant but if it is deemed significant there are methods available that can recover this chronological [41]. Real-life data for our analysis were obtained from [38].

This problem was modeled using GAMS 24.0 and solved using the CPLEX 12.0 solver. All simulations are conducted using an HP Z820 workstation with two E5-2687W processors clocked at 3.1 GHz.

B. Discussion of Numerical Results

In the course of the analysis, five different cases are considered, Cases A through to Case E. Case A is the baseline system with no BESS and conventional power plants are not flexible enough to deal with the fluctuations in RE production. The lack of flexibility was considered by using the lower bound of energy production from each generator. Case B is similar to Case A, except that has BESS deployed. Case C assumes no BESS deployment but is increases the flexibility of the conventional power plants using a "game-changing" mechanism, which increases the plant flexibility. Two case studies were considered in this article. Case D also assumes the deployment of BESS and the increased flexibility of the conventional generators with the main difference being that Case D uses an upper limit of 80% systemwide nonsynchronous generation (SNSP). Case E removes the limit imposed on SNSP in Case D. SNSP is calculated as the proportion of RE production plus the amount of power imported to the sum of the demand plus the amount of power exported over an hourly time period, as shown in (21).

TABLE VIII
COMPARISON OF SYSTEMWIDE COST TERMS AND ENERGY LOSSES ON AN ANNUAL BASIS

	Cases				
	A	B	C	D	E
Expected cost of O&M (M€/year)	734	715	695	679	676
Expected cost of PNS (M€/ year)	0	0	0	0	0
Cost of emissions (M€/ year)	237	226	212	204	204
Expected total cost (M€/ year)	971	941	908	883	880
Expected energy losses (TWh/ year)	0.63	+1.3%	+6.3%	+7.4%	+8.4%

Each of the cases is briefly summarized as follows.

1) Case A: No BESS deployed, nonflexible conventional power generation plants, and 80% SNSP limit.
2) Case B: BESSs deployed, nonflexible conventional power generation plants, and 80% SNSP limit.
3) Case C: No BESS deployed, flexible conventional power generation fleet, and 80% SNSP limit.
4) Case D: BESSs deployed, flexible conventional power generation fleet, and 80% SNSP limit.
5) Case E: BESSs deployed, flexible conventional power generation fleet, and no SNSP limit.

The expected systemwide costs and energy losses of the various cases are presented in Table VIII. The benefits of using BESS are evident in the table and these benefits are increased if the BESSs are combined with flexible conventional power plants.

Comparing the results from Case A and Case B, the introduction of BESS leads to a reduction in total costs of 3.1%, operation, and maintenance costs are reduced by 2.59% and emission costs are down 4.64%. Increasing the flexibility of the conventional power plants leads to a decrease of 6.5% in overall costs between Case A and Case C. Similar cost reduction can be seen for all cases with Cases B, D, and E showing a decline of 3%, 9%, and 9.4%, respectively. Deploying BESSs have the largest effect on these cost reductions. Removing the SNSP limit does not have a significant impact on the costs but this might vary according to different networks.

The introduction of the game-changing flexibility measures applied to the conventional power plants in Case C results in a decrease of 6.5% in overall costs between Case A and Case C. Comparing the flexibility measures introduced in Case C to the

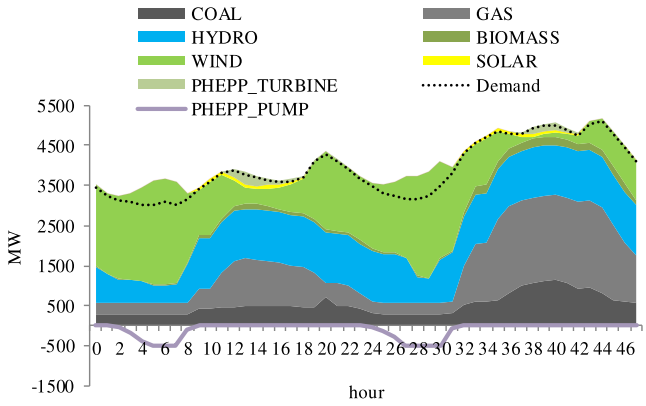

Fig. 2. Power production mix profile in Case A.

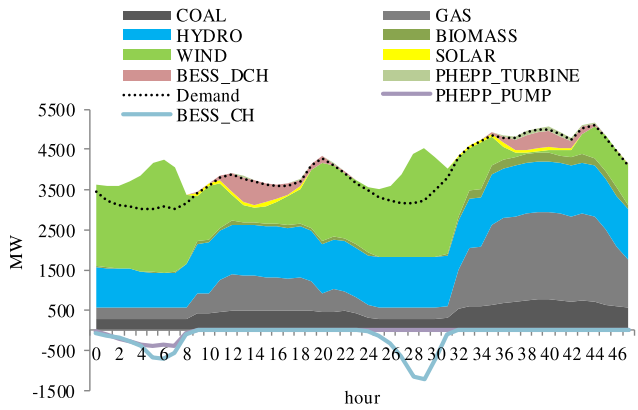

Fig. 3. Power production mix profile in Case B.

impact of BESS in Case B, the total costs are 0.41% lower in Case C than Case B. This is mainly due to the reduced emission and operation costs of Case C compared to Case B. Case D, which introduced the increased flexibility measures as well as BESS, led to a decrease in the total costs of 2.75% compared to Case C (with no BESS).

Comparing the results of Cases A–D, the full effect of the increased flexibility as well as the BESS can be seen. These effects lead to a 9.06% reduction in costs compared to Case A; however, there was an increase in the cost of the losses. Removing the SNSP constraint (as done in Case E) leads to a further reduction in total costs by 0.34% compared to Case D. This is due to lower operation and maintenance costs.

These results clearly show the benefit of BESS and increased system flexibility. The use of BESS increased the utilization and efficiency of RES while decreasing system costs. Costs were lowered by as much as 10% through the use of BESS. A further reduction in costs was seen when the SNSP constraint was relaxed. This shows that using both technologies in tandem reaps the highest benefits as they can work together to reduce system costs.

An interesting result is identified when looking at the energy losses given in Table VIII. The energy losses generally increase from Case A to Case E. If the value of the energy losses of Case A (0.63 TWh) is taken as a reference, then Cases B–E show an increase in the energy loses of 1.3%, 6.3%, 7.4%, and 8.4%, respectively. This result can be explained by the increased transmission losses in the lines as more RE is used, which is based far from the load centers. The extra losses are not as significant as the operational costs and costs of emissions offset the energy losses.

Profiles of the energy mix for Case A, Case B, Case C, Case D, and Case E are shown in Figs. 2–6, respectively. In the energy mix of Case B, as shown in Fig. 3, it can be seen that the majority of the generation comes from the combination of wind energy, hydroelectric plants, and gas-fired generation, which is the lowest contribution to the energy mix from biomass and solar PV. This is consistent with the energy mix in Case A but in Case B, there is an increase in clean energy sources and a decrease in conventional power plants due to the introduction of BESS.

This trend of lower generation from conventional power plants is again evident in Fig. 4, which is the energy mix for Case C.

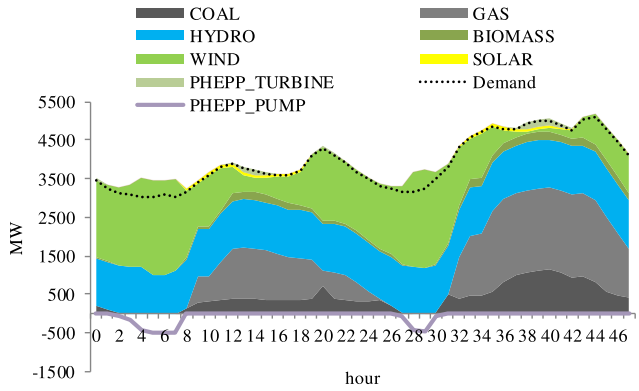

Fig. 4. Power production mix profile in Case C.

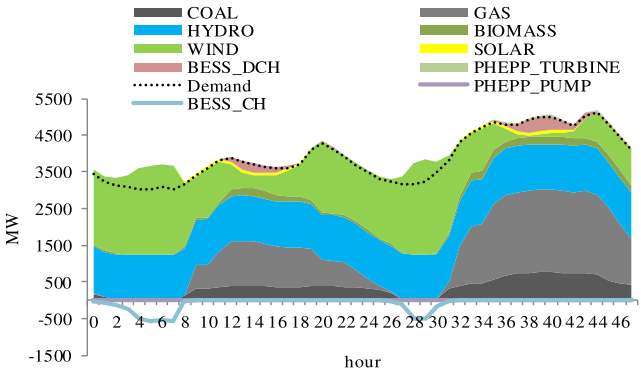

Fig. 5. Power production mix profile in Case D.

When generation exceeds demand, mostly when there is a large amount of wind generation, the pumping stations are activated.

The trend of lower conventional generation is reversed in Case D, Fig. 5, where there is a slight increase in gas generation in comparison to Case C but coal generation is reduced in Case D when compared to Case C. The remaining generation technologies remain largely the same with some small fluctuations in supply. The usage of BESS in Case D is also lower than in Case B. This is because there is the second source of flexibility, which is the game-changing mechanisms, present in Case D compared

TABLE IX
TOTAL RATE OF EACH TYPE OF POWER GENERATION AND LOSSES IN THE SYSTEM FOR A 48 h PERIOD

	Cases					
	A		B		C	
	Power [MW]	Share	Power [MW]	Share	Power [MW]	Share
Wind	64347.27	32.95%	63028.24	33.54%	61516.49	32.73%
Hydro	55345.78	28.34%	57204.27	30.44%	58950.91	31.37%
Gas	48891.88	25.04%	45288.63	24.10%	44923.36	23.91%
Coal	25822.21	13.22%	22260.01	11.85%	19572.30	10.41%
Biomass	5062.7	2.59%	4744.37	2.52%	5653.97	3.01%
Solar	1386.08	0.71%	1386.08	0.74%	1417.82	0.75%
Turbine	2084.55	1.07%	811.18	0.43%	1372.24	0.73%
Pumping	-4771.95	2.44%	-2216.79	-1.18%	-3195.84	1.70%
ESSs Charge	NA	NA	-7486.36	-3.98%	NA	NA
ESSs Discharge	NA	NA	5788.15	3.08%	NA	NA
Losses	2820.95	1.50%	2961.20	1.58%	2961.20	1.58%

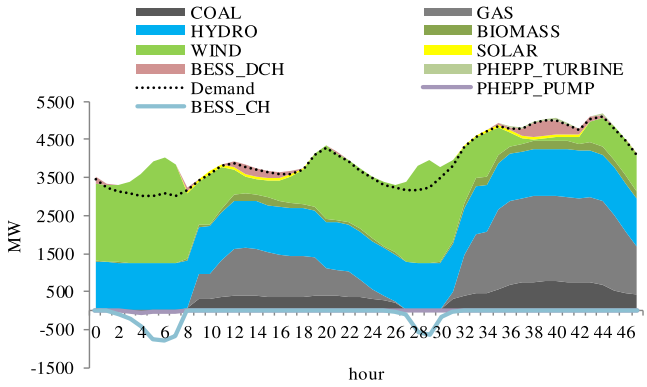

Fig. 6. Power production mix profile in Case E.

TABLE X
TOTAL RATE OF EACH TYPE OF POWER GENERATION AND LOSSES IN THE SYSTEM FOR 48 h CASE D AND E)

	D		E	
	Power [MW]	Share	Power [MW]	Share
Wind	62000.15	32.99%	62878.00	33.46%
Hydro	59859.35	31.85%	59810.89	31.83%
Gas	45809.38	24.38%	45847.22	24.40%
Coal	16737.39	8.91%	16461.55	8.76%
Biomass	5596.75	2.98%	5467.21	2.91%
Solar	1417.75	0.75%	1417.85	0.75%
Turbine	283.61	0.15%	349.63	0.19%
Pumping	0.00	0.00%	-219.46	0.12%
ESSs Charge	-4038.00	2.15%	-4521.17	2.41%
ESSs Discharge	3035.51	1.75%	3291.83	1.75%
Losses	2777.59	1.48%	2859.33	1.52%

to Case B. Finally, Case E is presented in Fig. 6 with no SNSP limit.

From the figures, it is clear to see that deploying BESS leads to better management of the variable RE production (especially wind) by storing it during periods of high generation but low demand. The energy mixes of Case A, Case B, and Case C are given in Table IX for a continuous period of 48 h. The results show a decrease in the use of conventional generation when compared to Case A and Case B, while the amount of RE production increased relative to Case A and Case B, except wind generation which decreased slightly when compared to Case B.

Table X represents the contribution of BESSs in Case E increased from 1.62% to 1.75% compared to Case D. This due to the relaxation of the SNSP in Case E. Therefore, since there is a greater integration of renewable energy in the network, there is greater availability of resources to store and also a greater need for flexibility in the network, which is provided by the use of BESSs. The results showed that BESS can provide larger than expected benefits to the Portuguese Transmission Network. This was done by increasing the flexibility of the transmission system, which allowed for better management of intermittent RE and this led to an overall increase in the efficiency of the transmission system.

A comparison of the two types of storage technologies, BESS and pumped hydro, is shown in Fig. 7. From the figure, it is clear to see that BESSs have a much higher rate of utilization.

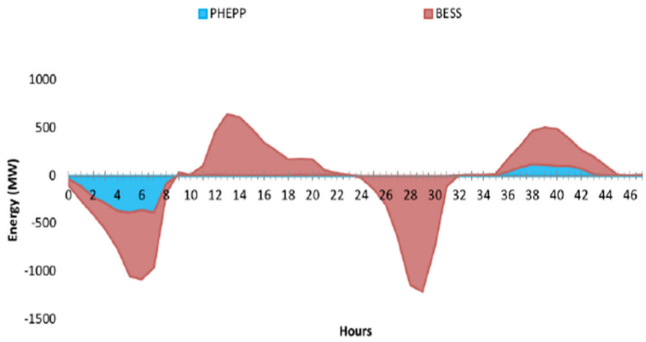

Fig. 7. Comparison between the two ESS technologies in Case B.

BESS provides a larger cost saving than pumped hydro, and thus, BESSs are the preferred ESS type in the model. BESS also leads to better management of high penetrations of RE production (especially wind energy) as BESS can store the energy in periods of high production and discharge the energy during periods of low generation or high demand.

Also, BESS can be deployed throughout the system more easily and more optimally sized when compared to pumped hydro energy storage systems. The BESSs provide a high total of the total system, with 3.08% in Case B. Thus, BESSs provide the transmission grid with the necessary flexibility to adequately

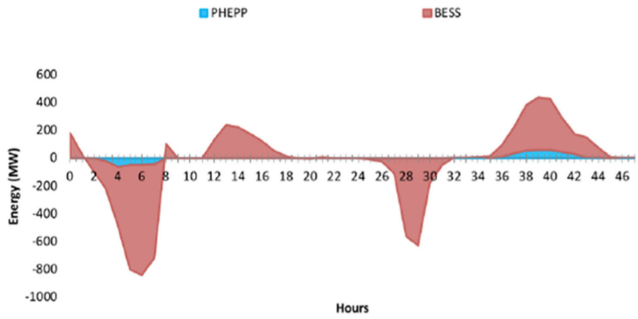

Fig. 8. Comparison between the two ESS technologies in Case E.

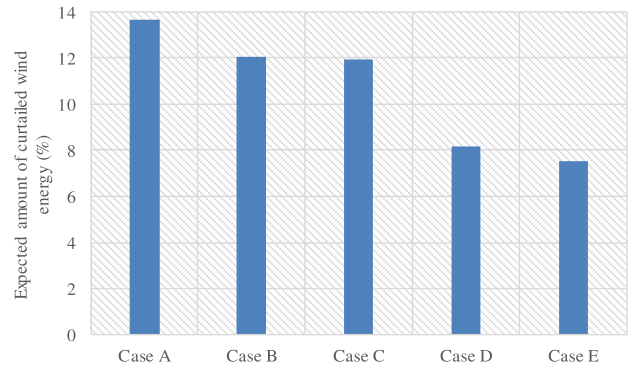

Fig. 9. Impacts on level of curtailed wind energy.

manage high proportions of RE production. Further comparison of BESS against pumped hydro in case E is shown in Fig. 8.

The increased penetration of SNSP was thought to require an increase in all available energy storage systems but there is still a clear preference for BESS in the system. This is further given in Table X with only a slight increase in pumped hydro capacity between the cases. Portugal's largest intermittent RES is wind energy. In some instances, generation exceeds demand and some generations must be curtailed if there are not suitable flexibility mechanisms available. In Portugal, the curtailed energy is generally from wind energy. The amount of curtailed energy from wind generation in each of the cases in the model is shown in Fig. 9.

A general trend can be seen, that is increasing the system flexibility (either through installing BESS, increasing the flexibility of the generators, or relaxing the SNSP constraints) leads to a lower amount of wind energy being curtailed. The amount of curtailed wind energy is 13.67% in Case A and this decreased to 12.04% in Case B. Case C has a value of 11.94% of wind energy curtailment, a total reduction of 12.66% compared to Case A. In Case D where the BESS and game-changing mechanisms are introduced the wind, energy curtailment is reduced to 8.16% of total wind energy representing a decrease of 40.3% compared to Case A. Relaxing the SNSP constraint further, as done in Case E, reduces the curtailment to 7.51%. The reduction in total costs and RES curtailment when the SNSP constraint is relaxed, thus reducing the amount of inertia in the system and this finding is consistent with the existing literature [18].

IV. Conclusion

The economic and technical potential of BESS to increase the operational flexibility of the Portuguese Transmission Network was studied in this article as a real case study. Intermittent RE generation and variable load were taken into account in the model used. The model used was a stochastic MILP which had the objective of minimizing costs subject to some economic and technical constraints. Also, the SNSP constraint was investigated in the model to examine the effects of a large penetration of RES on the stability of the power system. BESSs were optimally located and the analysis conducted used numerical results based on the Portuguese Transmission Network to investigate the effects of these BESS. The results showed that using BESS increased the efficiency of renewable energy generation and decreased the costs of operation. The costs decreased as much as 10% relative to a baseline scenario. Costs decreased further when the SNSP constraint was relaxed. The amount of wind energy curtailment also decreased with BESS deployment and curtailment was reduced further when the higher levels of SNSP were allowed. Energy losses are slightly increased with increasing BESS deployment, but these losses are due to the larger transmission line losses as more renewable energy is used which is based far away from load centers. The savings in operational costs and emissions completely offset this slight increase in transmission losses. The results showed that BESS can provide larger than expected benefits to the Portuguese Transmission Network, especially as it increased the flexibility of the transmission system, which allowed for better management of intermittent RE and an overall increase in the efficiency of the transmission system. The findings and conclusions of this article could be applied to several aspects of the power system. Developers of BESS plants as well as energy policy makers in Portugal will benefit from this article. The increase of the SNSP does bring additional challenges and costs for the power system for the system operator to balance supply and demand. BESS can provide solutions to these challenges.

References

[1] E. M. Carlini, R. Schroeder, J. M. Birkebæk, and F. Massaro, "EU transition in power sector: How RES affects the design and operations of transmission power systems," *Electr. Power Syst. Res.*, vol. 169, pp. 74–91, 2019.

[2] J. Wang, J. Wei, Y. Zhu, and X. Wang, "The reliability and operational test system of a power grid with large-scale renewable integration," *CSEE J. Power Energy Syst.*, vol. 6, no. 3, pp. 704–711, Sep. 2020.

[3] W. Tan, M. Shaaban, and M. Z. A. A. Kadir, "Stochastic generation scheduling with variable renewable generation: Methods, applications, and future trends," *Transm. Distrib. IET Gener.*, vol. 13, no. 9, pp. 1467–1480, 2019.

[4] S. R. Sinsel, R. L. Riemke, and V. H. Hoffmann, "Challenges and solution technologies for the integration of variable renewable energy sources—A review," *Renew. Energy*, vol. 145, pp. 2271–2285, Jan. 2020.

[5] M. R. M. Cruz, D. Z. Fitiwi, S. F. Santos, S. J. P. S. Mariano, and J. P. S. Cataláo, "Multi-flexibility option integration to cope with large-scale integration of renewables," *IEEE Trans. Sustain. Energy*, vol. 11, no. 1, pp. 48–60, Jan. 2020.

[6] Y. Li, Y. Chi, H. Tang, and C. Liu, "Study on characteristics of wind power transmission system with series compensation," *J. Eng.*, vol. 2019, no. 16, pp. 3333–3336, 2019.

[7] T. M. Gür, "Review of electrical energy storage technologies, materials and systems: Challenges and prospects for large-scale grid storage," *Energy Environ. Sci.*, vol. 11, no. 10, pp. 2696–2767, Oct. 2018.

[8] W.-P. Schill, "Electricity storage and the renewable energy transition," *Joule*, vol. 4, no. 10, pp. 2059–2064, Oct. 2020.

[9] M. Kazemi, H. Zareipour, N. Amjady, W. D. Rosehart, and M. Ehsan, "Operation scheduling of battery storage systems in joint energy and ancillary services markets," *IEEE Trans. Sustain. Energy*, vol. 8, no. 4, pp. 1726–1735, Oct. 2017.

[10] J. Villar, R. Bessa, and M. Matos, "Flexibility products and markets: Literature review," *Electr. Power Syst. Res.*, vol. 154, pp. 329–340, Jan. 2018.

[11] H. Zhu *et al.*, "Energy storage in high renewable penetration power systems: Technologies, applications, supporting policies and suggestions," *CSEE J. Power Energy Syst.*, pp. 1–9, 2020.

[12] A. Bagheri, V. Vahidinasab, and K. Mehran, "A novel multiobjective generation and transmission investment framework for implementing 100% renewable energy sources," *IET Gener., Transmiss. Distrib.*, vol. 12, no. 2, pp. 455–465, 2018.

[13] S. J. Davis *et al.*, "Net-zero emissions energy systems," *Science*, vol. 360, no. 6396, Jun. 2018, Art. no. eaas9793.

[14] European Comission, "A European green deal," Jan. 2020. Accessed: Sep. 29, 2020. [Online]. Available: https://ec.europa.eu/info/strategy/priorities-2019-2024/european-green-deal_en

[15] Ministry of Environment Climate Change, "National energy and climate plan 2030," 2019. [Online]. Available: https://www.portugal.gov.pt/pt/gc22/comunicacao/comunicado?i=plano-nacional-energia-e-clima-2030-aprovado-em-conselho-de-ministros

[16] A. R. de Oliveira *et al.*, "Joint analysis of the Portuguese and Spanish NECP for 2021-2030," in *Proc. 17th Int. Conf. Eur. Energy Market*, Sep. 2020, pp. 1–6.

[17] A. Nikoobakht, J. Aghaei, M. Shafie-khah, and J. P. S. Catalão, "Allocation of fast-acting energy storage systems in transmission grids with high renewable generation," *IEEE Trans. Sustain. Energy*, vol. 11, no. 3, pp. 1728–1738, Jul. 2020.

[18] L. Mehigan, D. Al Kez, S. Collins, A. Foley, B. Ó'Gallachóir, and P. Deane, "Renewables in the European power system and the impact on system rotational inertia," *Energy*, vol. 203, Jul. 2020, Art. no. 117776.

[19] L. Wang, X. Xie, X. Dong, Y. Liu, and H. Shen, "Real-time optimisation of short-term frequency stability controls for a power system with renewables and multi-infeed HVDCs," *IET Renew. Power Gener.*, vol. 12, no. 13, pp. 1462–1469, 2018.

[20] Y. Sun, Z. Zhao, M. Yang, D. Jia, W. Pei, and B. Xu, "Overview of energy storage in renewable energy power fluctuation mitigation," *CSEE J. Power Energy Syst.*, vol. 6, no. 1, pp. 160–173, Mar. 2020.

[21] S. D. Ahmed, F. S. M. Al-Ismail, M. Shafiullah, F. A. Al-Sulaiman, and I. M. El-Amin, "Grid integration challenges of wind energy: A review," *IEEE Access*, vol. 8, pp. 10857–10878, 2020.

[22] H. Shin and J. Hur, "Optimal energy storage sizing with battery augmentation for renewable-plus-storage power plants," *IEEE Access*, vol. 8, pp. 187730–187743, 2020.

[23] A. R. Dehghani-Sanij, E. Tharumalingam, M. B. Dusseault, and R. Fraser, "Study of energy storage systems and environmental challenges of batteries," *Renew. Sustain. Energy Rev.*, vol. 104, pp. 192–208, Apr. 2019.

[24] C. Crampes and J.-M. Trochet, "Economics of stationary electricity storage with various charge and discharge durations," *J. Energy Storage*, vol. 24, 2019, Art. no. 100746.

[25] Y. Li, J. Wang, C. Gu, J. Liu, and Z. Li, "Investment optimization of grid-scale energy storage for supporting different wind power utilization levels," *J. Mod. Power Syst. Clean Energy*, vol. 7, no. 6, pp. 1721–1734, Nov. 2019.

[26] X. Deng and T. Lv, "Power system planning with increasing variable renewable energy: A review of optimization models," *J. Clean. Prod.*, vol. 246, Feb. 2020, Art. no. 118962.

[27] M. J. M. Al Essa, "Power management of grid-integrated energy storage batteries with intermittent renewables," *J. Energy Storage*, vol. 31, Oct. 2020, Art. no. 101762.

[28] C. Zhang, H. Cheng, L. Liu, H. Zhang, X. Zhang, and G. Li, "Coordination planning of wind farm, energy storage and transmission network with high-penetration renewable energy," *Int. J. Electr. Power Energy Syst.*, vol. 120, Sep. 2020, Art. no. 105944.

[29] N. E. Koltsaklis and A. S. Dagoumas, "State-of-the-art generation expansion planning: A review," *Appl. Energy*, vol. 230, pp. 563–589, Nov. 2018.

[30] H. Nemati, M. A. Latify, and G. R. Yousefi, "Optimal coordinated expansion planning of transmission and electrical energy storage systems under physical intentional attacks," *IEEE Syst. J.*, vol. 14, no. 1, pp. 793–802, Mar. 2020.

[31] X. Yan, C. Gu, X. Zhang, and F. Li, "Robust optimization-based energy storage operation for system congestion management," *IEEE Syst. J.*, vol. 14, no. 2, pp. 2694–2702, Jun. 2020.

[32] J. Graça Gomes, J. Medeiros Pinto, H. Xu, C. Zhao, and H. Hashim, "Modeling and planning of the electricity energy system with a high share of renewable supply for portugal," *Energy*, vol. 211, Nov. 2020, Art. no. 118713.

[33] S. Wang, G. Geng, and Q. Jiang, "Robust co-planning of energy storage and transmission line with mixed integer recourse," *IEEE Trans. Power Syst.*, vol. 34, no. 6, pp. 4728–4738, Nov. 2019.

[34] A. Bera *et al.*, "Maximising the investment returns of a grid-connected battery considering degradation cost," *IET Gener. Transmiss. Distrib.*, vol. 14, no. 21, pp. 4711–4718, 2020.

[35] M. Martin Almenta, D. J. Morrow, R. J. Best, B. Fox, and A. M. Foley, "An analysis of wind curtailment and constraint at a nodal level," *IEEE Trans. Sustain. Energy*, vol. 8, no. 2, pp. 488–495, Apr. 2017.

[36] M. Ahmadi, M. E. Lotfy, R. Shigenobu, A. M. Howlader, and T. Senjyu, "Optimal sizing of multiple renewable energy resources and PV inverter reactive power control encompassing environmental, technical, and economic issues," *IEEE Syst. J.*, vol. 13, no. 3, pp. 3026–3037, Sep. 2019.

[37] D. Z. Fitiwi, L. Olmos, M. Rivier, F. de Cuadra, and I. J. Pérez-Arriaga, "Finding a representative network losses model for large-scale transmission expansion planning with renewable energy sources," *Energy*, vol. 101, pp. 343–358, Apr. 2016.

[38] "Mada da RNT," Rede Electrica Nacional, 2016. [Online]. Available: http://www.centrodeinformacao.ren.pt/PT/InformacaoTecnica/PublishingImages/Mapa-REN-2016-MEDIUM.jpg

[39] "Caracterização da rede nacional de transporte para efeitos de acesso à rede," Rede Eléctrica Nacional, Lisboa, Março, p. 16, 2017.

[40] M. P. S. Pereira, D. Z. Fitiwi, S. F. Santos, and J. P. S. Catalão, "Managing RES uncertainty and stability issues in distribution systems via energy storage systems and switchable reactive power sources," in *Proc. IEEE Int. Conf. Environ. Elect. Eng./IEEE Ind. Commercial Power Syst. Europe*, Jun. 2017, pp. 1–6.

[41] R. Khatami, M. Parvania, and P. P. Khargonekar, "Scheduling and pricing of energy generation and storage in power systems," *IEEE Trans. Power Syst.*, vol. 33, no. 4, pp. 4308–4322, Jul. 2018.